ADVANCES IN ATMOSPHERIC SCIENCES, VOL. 31, MARCH 2014, 449–456

New Evidence for Improving Omega Estimation by Explicitly Considering Horizontal Divergence

YUAN Zhuojian*[1], QI Jindian[1], GAO Shouting[2], FENG Yerong[3], XU Pengcheng[4], and WU Naigeng[3]

[1]*Center for Monsoon and Regional Environment/Department of Atmospheric Science, Sun Yat-sen University, Guangzhou* 510275

[2]*Laboratory of Cloud-Precipitation Physics and Severe Storms, Institute of Atmospheric Physics, Chinese Academy of Sciences, Beijing* 100029

[3]*Guangdong Meteorological Observatory, Guangzhou* 510080

[4]*Institute of Applied Mathematics, Academy of Mathematics and Systems Sciences, Chinese Academy of Sciences, Beijing* 100190

(Received 4 January 2013; revised 20 May 2013; accepted 12 August 2013)

ABSTRACT

It is well known that the quasi-geostrophic (QG) omega equation with only two contributors respectively associated with vorticity advection (VA) and temperature advection is derived for midlatitude synoptic-scale systems only. Based on reliable reanalysis data, new evidence revealed by cyclonic and anticyclonic cases indicates that forecasters might sometimes experience problems by paying too much attention to the 500-hPa VA when estimating vertical motions not only in subtropical systems but also in systems meeting all the assumptions of the QG omega equation. Our investigations also showed that explicitly considering the vertical profiles of horizontal divergence could allow for better interpretation of vertical motions and weather in these real cases, suggesting that this equation might not be sufficient due to the presence of only two horizontal-divergence-related (HDR) mechanisms and the absence of other HDR mechanisms, e.g., frictional force, mountain barriers, diabatic/adiabatic processes, and acceleration/deceleration of air flows.

Key words: omega estimation, weather forecast, horizontal divergence, vertical motion

Citation: Yuan, Z. J., J. D. Qi, S. T. Gao, Y. R. Feng, P. C. Xu, and N. G. Wu, 2014: New evidence for improving omega estimation by explicitly considering horizontal divergence. *Adv. Atmos. Sci.*, **31** (2), 449–456, doi: 10.1007/s00376-013-3003-5.

1. Introduction

It is necessary for scientists to pay great attention to the vertical motion (e.g., ω in isobaric coordinates) because flood/drought and all weathers are associated with vertical transport of vapor driven by vertical motion. However, ω is too weak for reliable measurement (Smith, 1971). Thus, a very important theory—the quasi-geostrophic (QG) theory, with the QG omega ($\omega_{\rm QG}$) equation as one of the great outcomes—was developed for the evolution of weather systems. Following its development, the $\omega_{\rm QG}$ equation has been included in all dynamic-meteorology textbooks worldwide as the popular approach for ω estimation. In the $\omega_{\rm QG}$ equation,

$$\left(\nabla^2+\frac{f_0^2}{\sigma}\frac{\partial^2}{\partial p^2}\right)\omega=\frac{f_0}{\sigma}\frac{\partial}{\partial p}\left[\boldsymbol{V}_{\rm g}\cdot\nabla\left(\frac{1}{f_0}\nabla^2\Phi+f\right)\right]+\frac{1}{\sigma}\nabla^2\left[\boldsymbol{V}_{\rm g}\cdot\nabla\left(-\frac{\partial\Phi}{\partial p}\right)\right], \quad (1)$$

there are only two right-hand-side (RHS) terms used to determine ω on the left hand side (LHS) of Eq. (1). One is the vertical derivative of vorticity ($\zeta\approx\zeta_{\rm g}=\nabla^2\Phi/f_0$) advection (VA); and the other is the Laplacian of temperature advection (TA), where $\boldsymbol{V}_{\rm g}$ is the geostrophic portion of horizontal velocity ($\boldsymbol{V}_2$ with the subscript 2 representing two dimensions), Φ is the geopotential, $f=2\Omega\sin\varphi$ is the Coriolis parameter, $f_0=2\Omega\sin 45^\circ$ is a constant for midlatitude systems, σ is the static stability parameter, p is the air pressure, and $\Omega=7.292\times10^{-5}$ s^{-1} is the angular speed of rotation of the Earth (Holton, 1979, p. 136). Obviously, the contribution of horizontal divergence ($\nabla\cdot\boldsymbol{V}_2$) to $\omega_{\rm QG}$ is not explicitly involved in Eq. (1) as a RHS term.

With $\nabla^2\omega\propto-\omega$ (Holton, 1979, p. 137, 2004, p. 166), the qualitative content of the $\omega_{\rm QG}$ equation is summarized by Holton (1979, p. 140) as:

"Omega Equation

$$\binom{\text{Sinking}}{\text{Rising}}\text{ motion }\propto\text{ Rate of increase with height of }(\pm)\text{ vorticity advection}+\binom{\text{cold}}{\text{warm}}\text{advection}". \quad (2)$$

* Corresponding author: YUAN Zhuojian
Email: qianyk@mail3.sysu.edu.cn

© Institute of Atmospheric Physics/Chinese Academy of Sciences, and Science Press and Springer-Verlag Berlin Heidelberg 2014

Based on Eq. (2), the 500-hPa negative vorticity advection (NVA) responsible for the lower-layer descent and the 500-hPa positive VA for ascent are still widely taught and used in the meteorology community.

Since Eq. (2) and the 500-hPa NVA with the lower-layer descent are considered well understood and accepted, when the 500-hPa NVA (Figs. 1b and c) was observed before a severe rainstorm struck South China at 1800 UTC 6 May 2010 (Fig. 1a), severe-storm warnings were not issued. Unfortunately, at around midnight local time (1800 UTC 6 May 2010), a 99.1-mm h^{-1} rainfall event (Fig. 1a) suddenly flooded some downtown areas of Guangzhou (the capital city of Guangdong Province in South China), causing heavy losses. Although squall lines (not shown) and convective instability (Fig. 1g) with corresponding temperature advections (Fig. 1f) were considered in this forecast, the 500-hPa NVA with the low-layer descents had received the most attention [exactly as pointed out by Dunn (1991, p. 70)], not the $\nabla \cdot \boldsymbol{V}_2$ profiles. However, evidence revealed by reliable data (described in section 2) shows that, consistent with the severe rainstorm, the strong ascents (Fig. 1d) were accompanied by lower-layer convergence, $\nabla \cdot \boldsymbol{V}_2 < 0$, and upper-layer divergence, $\nabla \cdot \boldsymbol{V}_2 > 0$ (Fig. 1e), suggesting that an improvement of ω estimation should be made with significant atten-

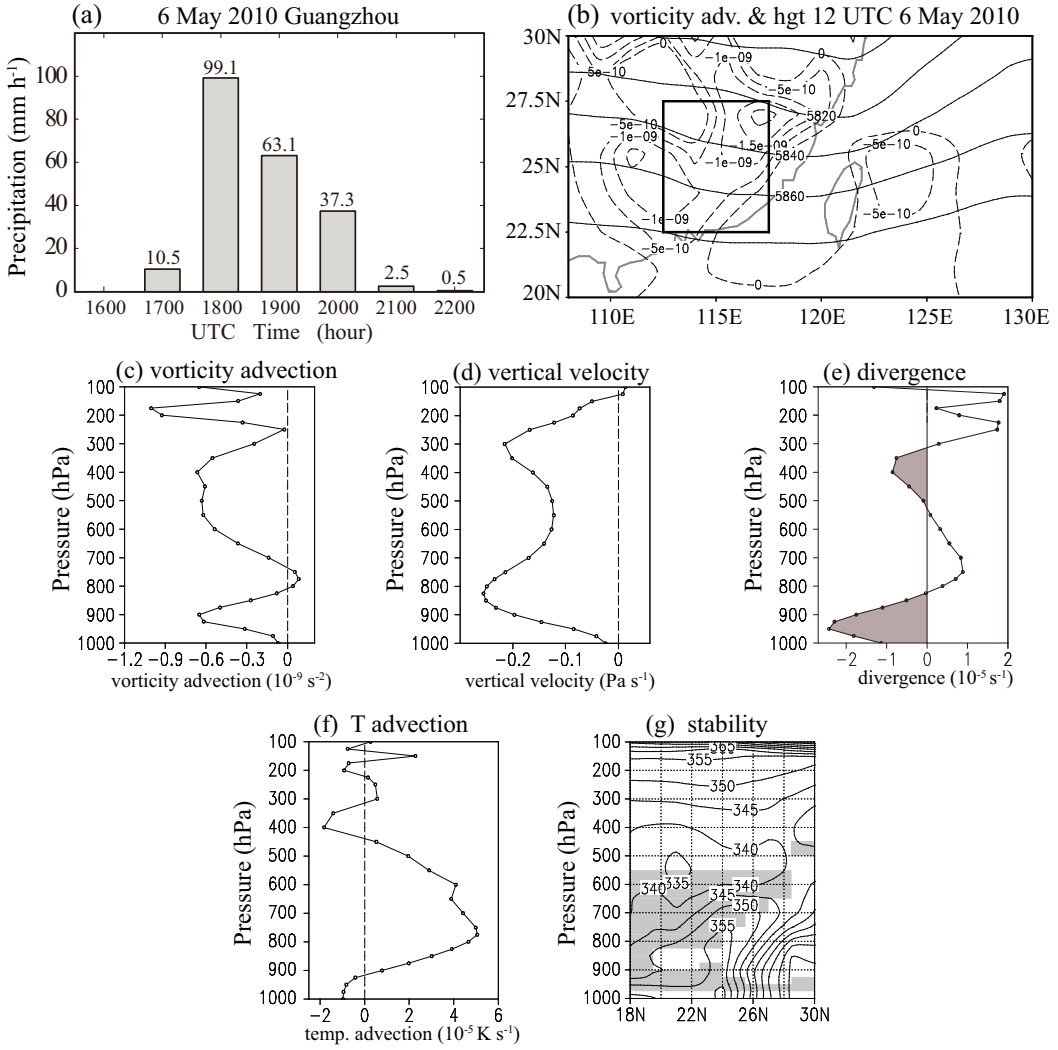

Fig. 1. Prior to the rainstorm with (a) 99.1 mm h^{-1} rainfall observed at 1800 UTC 6 May 2010 according to rain gauge measurements at Guangzhou weather station, some available weather conditions given here are: (b) the 500-hPa NVA ($-\boldsymbol{V}_2 \cdot \nabla\zeta < 0$, dashed line, interval of 5×10^{-10} s^{-2}) and geopotential height (solid line, interval of 20 gpm). The box indicates the (22.5°–27.5°N, 112.5°–117.5°E) region for regionally-averaged vertical profiles of (c) $-\boldsymbol{V}_2 \cdot \nabla\zeta \times 10^9$ s^{-2} with negative values representing NVA; (d) ω Pa s^{-1} with $\omega < 0$ representing ascent; (e) $\nabla \cdot \boldsymbol{V}_2 \times 10^5$ s^{-1} (with convergence $\nabla \cdot \boldsymbol{V}_2 < 0$, shaded); (f) $-\boldsymbol{V}_2 \cdot \nabla T \times 10^5$ K s^{-1} with $-\boldsymbol{V}_2 \cdot \nabla T > 0$ representing the warm advection; and (g) the vertical-meridional section of pseudo-equivalent potential temperature (θ_{se}) along 113°E, with the convective instability area shaded based on ERA-Interim reanalysis data for the 1200 UTC 6 May 2010 cyclone.

tion to $\nabla \cdot \boldsymbol{V}_2$ profiles.

In order to learn the lessons from this forecast and make weather forecasts better in future, the restrictions of the $\omega_{\rm QG}$ equation are briefly reviewed in section 3. Additional evidence is provided in section 4 for improving the ω estimation by considering the explicit contribution to ω of $\nabla \cdot \boldsymbol{V}_2$ profiles. A discussion and summary are given in section 5.

2. Data

The precipitation data used in the present study were obtained from the Guangdong Meteorological Observatory. Since we were unable to have access to higher resolution data for the 2010 case, the gridded data of geopotential, temperature, horizontal wind, vertical velocity, and specific humidity were from the European Centre for Medium-Range Weather Forecasts (ECMWF) Interim dataset (ERA-Interim) with a $1.5^\circ \times 1.5^\circ$ resolution and 6-h interval at 37 pressure levels from 1000 hPa to 1 hPa. These data were considered accurate enough for the main purpose of the study (i.e., reminding forecasters that sufficient attention should be paid to the assumptions of the $\omega_{\rm QG}$ equation for synoptic systems when using the 500-hPa vorticity advection to estimate the lower-layer vertical motion). An investigation of midlatitude synoptic-scale anticyclones was also carried out to alert forecasters to the possibility that sometimes the $\omega_{\rm QG}$ equation does not work well for systems meeting all the equation's assumptions. For selecting systems that met all the assumptions of the $\omega_{\rm QG}$ equation, the gridded data also included 40-yr (1957–2002) reanalysis data (ERA-40) of the ECMWF. This ERA-40 dataset has a $2.5^\circ \times 2.5^\circ$ resolution, 6-h interval, and 23 pressure levels from 1000 hPa to 10 hPa.

3. Brief review of the restrictions of the $\omega_{\rm QG}$ equation

Previous studies (e.g., Petterssen, 1956; Hoskins et al., 1978; Trenberth, 1978; Dunn, 1991; Viúdez et al., 1996) have pointed out that ω underestimation with Eq. (1) is unavoidable due to the cancellation between the two RHS terms. A $\boldsymbol{Q}$-vector form of the $\omega_{\rm QG}(\boldsymbol{Q} - \omega_{\rm QG})$ equation negates this two-term-cancellation problem through the combination of these two terms (e.g., Hoskins et al., 1978; Dunn, 1991, p. 70; Holton, 2004, 168–170). The assumptions used to build these $\omega_{\rm QG}$ equations include the disregard of the observed neutral stability ($\sigma = 0$) and static instability ($\sigma < 0$) due to the presence of σ as a denominator in Eq. (1) and in the new form of the $\omega_{\rm QG}$ equation $(N - \omega_{\rm QG})$ obtained by adding the Laplacian of the diabatic heating rate to Eq. (1) (Holton, 2004, p. 165), or σ as the coefficient of unknown ω in the $\boldsymbol{Q} - \omega_{\rm QG}$ equation and in the elliptic-type generalized ω equation (e.g., Pauley and Nieman, 1992). The assumption of $\sigma > 0$ is reasonable since Eq. (1), as well as the $\boldsymbol{Q} - \omega_{\rm QG}$ and $N - \omega_{\rm QG}$ equations, are derived only for midlatitude synoptic systems to make sure that these equations are elliptic-type diagnostic equations (e.g., Krishnamurti, 1968a, 1968b; Dutton, 1986, p. 362; Pauley and Nieman, 1992, p. 1113; Tan and Curry, 1993; Räisänen, 1995; Kim et al., 2006; Stone and Goldbart, 2008, 193–194). Thus, when these $\omega_{\rm QG}$ equations are applied to real cases, many studies have suggested that the observed $\sigma \leqslant 0$ should be removed through data modification. Such data modification could be that "static stability values less than 0.002 $\mathrm{m^{-2}s^{-2}mb^{-2}}$ are set equal to that value" (Pauley and Nieman, 1992, p. 1113), or the long-term averaged value (Kim et al., 2006). Räisänen (1995, Table 1) shows that to avoid $|\omega| \to \infty$, modifying the observed $\sigma \leqslant 0$ is necessary in tropical and extratropical systems at both 900 hPa and 300 hPa.

Even in midlatitude synoptic systems with $\sigma > 0$, the additional uncertainty could be introduced into the ω estimation by Eq. (1) through the calculation of the fourth-order derivatives in the RHS terms of Eq. (1) with finite difference schemes and gridded data, leading to a possible too-low signal-to-noise ratio in the results (e.g., Dunn, 1991; Press et al., 1992, p. 180). For example, based on the ERA-Interim reanalysis data from the ECMWF, the 500-hPa ζ field (Fig. 2b, dealing with the second-order derivative of Φ) at 1800 UTC 6 May 2010 was noisier than the corresponding Φ field (Fig. 2a). Therefore, the results of the RHS terms of Eq. (1) (dealing with the fourth-order derivative of Φ) could be much

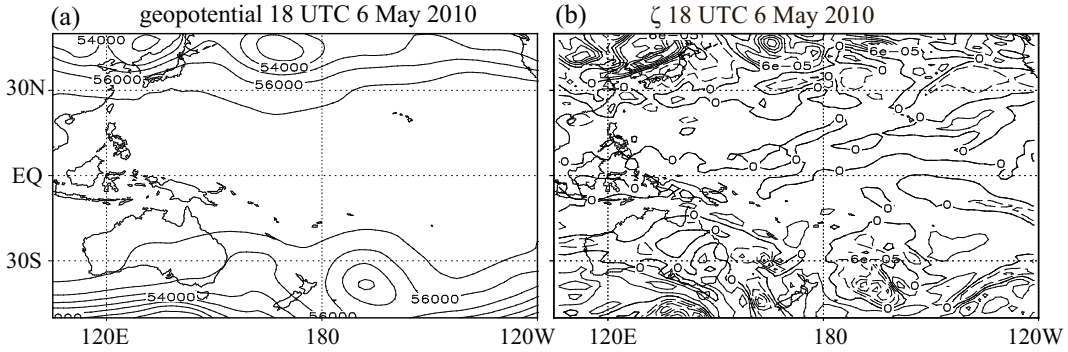

Fig. 2. (a) The 500-hPa Φ (interval of 1000 $\mathrm{m^2\ s^{-2}}$) and (b) relative vorticity (interval of $3 \times 10^{-5}\ \mathrm{s^{-1}}$) based on ERA-Interim reanalysis data for 1800 UTC 6 May 2010.

noisier.

4. Additional evidence for improving the omega estimation by explicitly considering the horizontal divergence

With the advantage of reanalysis data, this section focuses on the evidence that Eqs. (1) or (2) sometimes might not hold well even for midlatitude synoptic anticyclones with $\sigma > 0$ due to the absence of an explicit contribution of $\nabla \cdot \boldsymbol{V}_2$ on the RHS of Eq. (1). The evidence is revealed through a comparison between the LHS and RHS values of simplified equations [Eqs. (3) and (4), below] used to build Eqs. (1) or (2).

According to Holton (1979, 2004), the derivation of Eq. (1) starts by eliminating all ω terms in the primitive ζ equation (Holton, 1979, subsection 6.2.1, 126–130, 2004, 147–152) to generate the simplified ζ equation

$$\frac{\partial \zeta}{\partial t} + \boldsymbol{V}_2 \cdot \nabla(\zeta + f) = -f \nabla \cdot \boldsymbol{V}_2 \,, \tag{3}$$

after using the assumption $(\zeta + f) \approx f$ on the RHS of Eq. (3). Correspondingly, the primitive thermodynamic energy equation is also simplified as

$$\frac{\partial T}{\partial t} + \boldsymbol{V}_2 \cdot \nabla T = \frac{p\sigma}{R}\omega \,, \tag{4}$$

after using the following assumptions: (i) midlatitude synoptic systems are statically stable $(\sigma > 0)$ for the calculation of ω since the neutral stability $(\sigma = 0)$ will lead to $|\omega| \to \infty$; (ii) midlatitude synoptic systems are approximately adiabatic since the LHS terms of Eq. (4), respectively associated with temperature tendency, $\partial T/\partial t$, and TA, are larger than the diabatic term (Holton, 1979, 127–128). Based on the further simplified Eqs. (3) and (4) with the QG theory, Eq. (1) is derived through eliminating the $\partial T/\partial t$ and $\partial \zeta/\partial t$ terms (Holton, 1979, subsections 6.2.2–6.3, 126–143), leading to ω being determined only by VA and TA processes.

The following quantitative comparisons between the LHS and RHS values of Eqs. (3) and (4) are made with the ERA-40 reanalysis data for the real anticyclones selected that satisfied all the assumptions used in the derivation of Eqs. (1)

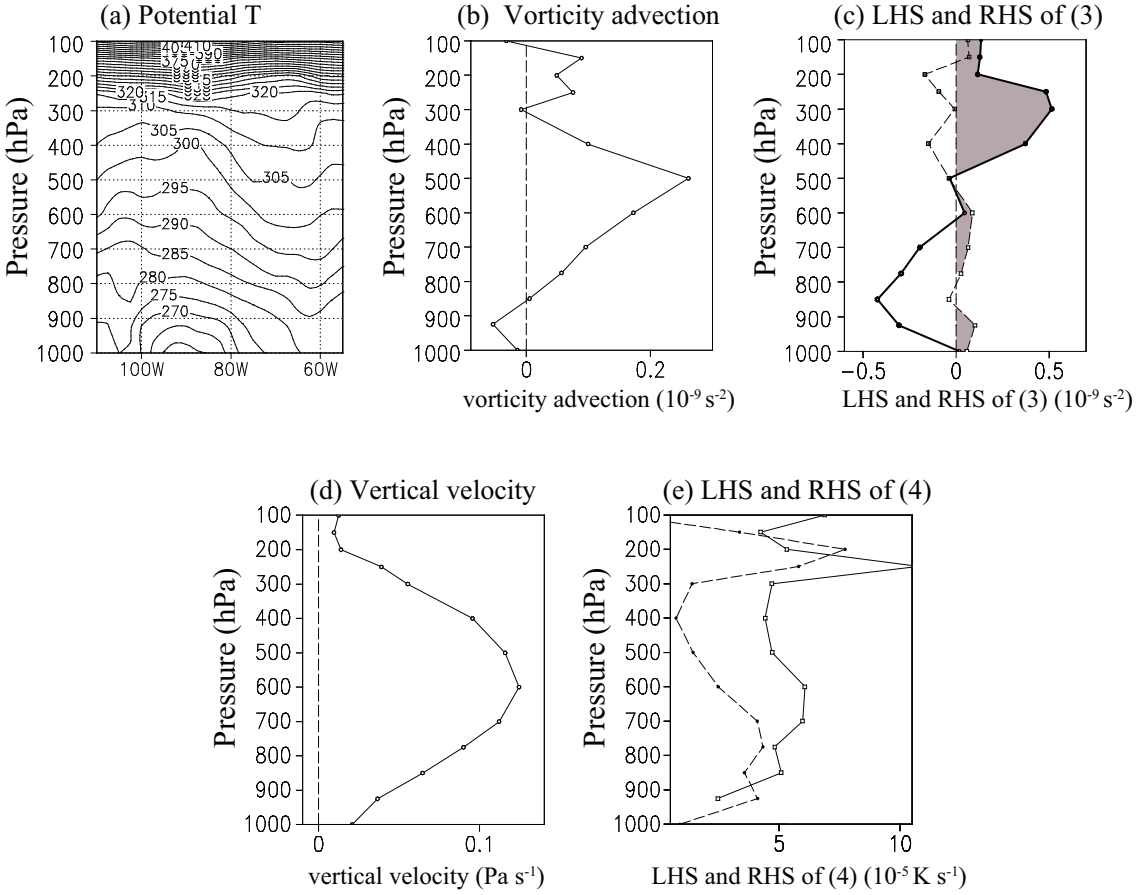

Fig. 3. (a) The vertical-zonal section of potential temperature along 40°N latitude. The (37°–43°N, 100°–95°W) regionally-averaged vertical profiles of: (b) $\boldsymbol{V}_2 \cdot \nabla(\zeta + f) \times 10^9$ s^{-2} with $-\boldsymbol{V}_2 \cdot \nabla(\zeta + f) < 0$ or $\boldsymbol{V}_2 \cdot \nabla(\zeta + f) > 0$ representing the NVA; (c) $[\partial\zeta/\partial t + \boldsymbol{V}_2 \cdot \nabla(\zeta + f)] \times 10^9$ (s^{-2}, dashed line) and $-f\nabla \cdot \boldsymbol{V}_2 \times 10^9$ (s^{-2}, solid line) with the convergence, $f\nabla \cdot \boldsymbol{V}_2 < 0$ or $-f\nabla \cdot \boldsymbol{V}_2 > 0$, area shaded; (d) ω (Pa s^{-1}) with $\omega > 0$ representing descent; and (e) $(\partial T/\partial t + \boldsymbol{V}_2 \cdot \nabla T) \times 10^5$ (K s^{-1}, dashed line) and $p\sigma\omega/R \times 10^5$ (K s^{-1}, solid line) based on ERA-40 reanalysis data for the 1200 UTC 18 February 1978 extratropical anticyclone.

or (2). Figure 3 shows the midlatitude synoptic anticyclone affecting the (37°–43°N, 100°–95°W) region at 1200 UTC 18 February 1978 to be characterized by monotonous change with height of VA in the 950–500-hPa layer (Fig. 3b) in a cold dome without noticeable effects of $\sigma \leqslant 0$ (Fig. 3a). The RHS of Eq. (3) i.e., $-f\nabla\cdot\boldsymbol{V}_2$, displays the 500–200-hPa convergence ($\nabla\cdot\boldsymbol{V}_2<0$ or $-f\nabla\cdot\boldsymbol{V}_2>0$, indicated by the shaded area based on the solid profile in Fig. 3c) and 1000–600-hPa divergence ($\nabla\cdot\boldsymbol{V}_2>0$ or $-f\nabla\cdot\boldsymbol{V}_2<0$; Fig. 3c, solid line) with a significant downward motion ($\omega>0$) at 500 hPa (Fig. 3d, directly from the ERA-40 ω data). Noticeably, the LHS of Eq. (3) [i.e., $\partial\zeta/\partial t+\boldsymbol{V}_2\cdot\nabla(\zeta+f)$, calculated with the central difference scheme; Fig. 3c, dashed line] is opposite to the RHS of Eq. (3) (Fig. 3c, solid line) in this real anticyclone meeting all the QG assumptions. The 500–200-hPa weak "divergence" (Fig. 3c, dashed line) and the 1000–600-hPa weak "convergence" (the shaded area based on the dashed profile in Fig. 3c) indicate a weak "upward motion" around 500 hPa [referred to as VA-related weak ascent due to the absence of $\partial\zeta/\partial t$ and $\partial T/\partial t$ in Eq. (1) obtained by the combination of the further simplified Eqs. (3) and (4)].

To elucidate the contribution from the thermodynamic processes, similar quantitative comparisons were also made between the LHS and RHS values of Eq. (4). Figure 3e shows a relatively weak "downward motion" at 500 hPa due to the $\partial T/\partial t+V_2\cdot\nabla T$ (calculated with the central difference scheme) on the LHS of Eq. (4) (referred to as TA-related relatively-weak descent; Fig. 3e, dashed line) and a relatively strong "downward motion" due to the RHS of Eq. (4) (Fig. 3e, solid line, directly from the ERA-40 data).

Consistent with observations and previous studies (e.g., Petterssen, 1956; Hoskins et al., 1978; Trenberth, 1978; Dunn, 1991; Viúdez et al., 1996), there exists the cancellation between the VA-related weak ascent and the TA-related relatively-weak descent, leading to VA- and TA-related $\omega\approx 0$ around 500 hPa. Since there are only VA and TA terms on the RHS of Eq. (1), it might underestimate the ω around 500 hPa in this real anticyclone. This VA- and TA-related $\omega\approx 0$ around 500 hPa is quite different from the near-maximum downward motion around 500 hPa shown by Fig. 3d (directly from ERA-40 ω data). Similar to the 2010 heavy-rain case (Fig. 1), the $\nabla\cdot\boldsymbol{V}_2$ again interprets the ω profile and weather in the anticyclone well. The present cyclone and anticyclone case studies suggest that explicitly considering the contribution of $\nabla\cdot\boldsymbol{V}_2$ might improve the estimation of ω.

More midlatitude anticyclones that have caught meteorologists' attention can also be studied. For example, in the intense North American anticyclone during the winter of 1989, selected by Tan and Curry (1993), at 0600 UTC 29 January 1989 this midlatitude synoptic anticyclone was characterized by a (zonal span $\approx 5\times10^6$ m) cold dome with $\sigma\leqslant 0$ affecting the (175°E–135°W, 1000–850 hPa) region (Fig. 4a) and by non-monotonous change with height of VA in the 1000–500-hPa layer (Fig. 4b). Since these features do not meet the requirements of Eqs. (1) or (2), $\sigma\leqslant 0$ must be removed by data modification to avoid the divergent solution (Tan and Curry, 1993, p. 963). With the explicit contribution of $\nabla\cdot\boldsymbol{V}_2$, the $|\omega|\to\infty$ problem might be reduced because the mass conservation law guarantees a non-zero denominator and non-zero coefficient for ω determined by $\nabla\cdot\boldsymbol{V}_2$.

5. Discussion and summary

In the present case studies, several vortices (based on ECMWF reanalysis data) were examined to highlight two kinds of possibilities to forecasters. One is that using Eq. (1) to estimate the vertical motions in subtropical cyclones could lead to an underforecasting of rainfall since Eq. (1) (the $\boldsymbol{Q}-\omega_{\mathrm{QG}}$ equation or the $N-\omega_{\mathrm{QG}}$ equation) is derived only for midlatitude systems. The other is that using Eq. (1)

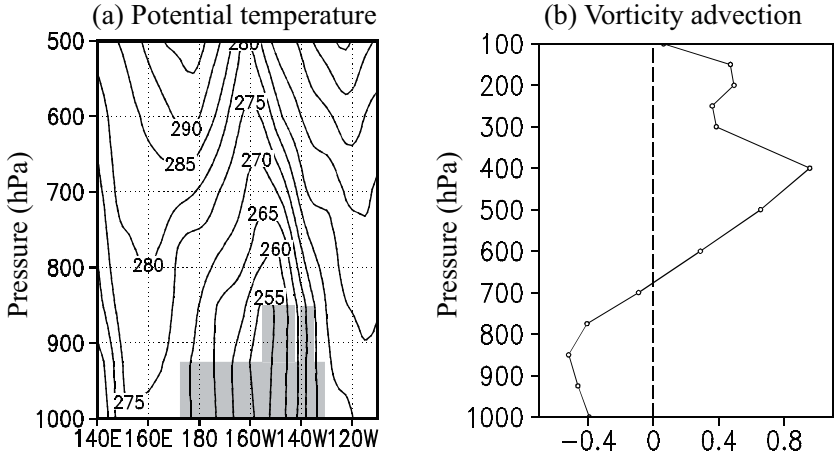

Fig. 4. (a) The vertical-zonal section of potential temperature along 55°N latitude (with neutral stability $\sigma=0$ and static instability $\sigma<0$ areas shaded) and (b) the (52.5°–57.5°N, 175°E–135°W) regionally-averaged vertical profiles of $\boldsymbol{V}_2\cdot\nabla(\zeta+f)\times10^9$ s^{-2} based on the ERA-40 reanalysis data for the 0600 UTC 29 January 1989 extratropical anticyclone.

to estimate vertical motions might result in $\omega \approx 0$ in the mid troposphere of midlatitude synoptic-scale anticyclones meeting all the QG assumptions. These cyclone and anticyclone case studies suggest that explicitly considering the vertical profiles of $\nabla \cdot \boldsymbol{V}_2$ should improve ω estimation because the vertical profiles of $\nabla \cdot \boldsymbol{V}_2$ reasonably match and interpret the ω profiles and weather in these real cases. Thus, the problems with Eq. (1) might be that it considers only VA and TA terms and neglects other mechanisms of $\nabla \cdot \boldsymbol{V}_2$.

To understand why Eq. (1) does not include the explicit contribution of $\nabla \cdot \boldsymbol{V}_2$ to ω, its derivation was reviewed. According to Holton (1979, 129–130, 2004, 151–152), in the derivation of Eq. (1), $-\nabla \cdot \boldsymbol{V}_2$ on the RHS of Eq. (3) is replaced by the undetermined $\partial\omega/\partial p$ for the purpose of determining ω with Eq. (3). Since observations show that $\nabla \cdot \boldsymbol{V}_2$ is associated with not only VA and TA, but also frictional force, mountain barriers, acceleration/deceleration of air flows, radiation heating/cooling, latent heating, latent heat flux, sensible heat flux etc., the replacement indicates that, with the modified ζ equation, the unknown $\partial\omega/\partial p$ is determined only by the vorticity terms on the LHS of Eq. (3). Holton's text also shows that the TA is introduced into the $\omega_{\rm QG}$ equation by eliminating the time derivations of vorticity and temperature through the combination of further simplified Eqs. (3) and (4). As a result, the contributions to $\partial\omega/\partial p$ from other ageostrophic processes are all neglected due to the disappearance of $\nabla \cdot \boldsymbol{V}_2$ in Eq. (3).

More importantly, with the replacement of $-\nabla \cdot \boldsymbol{V}_2$ on the RHS of Eq. (3) by $\partial\omega/\partial p$, the coefficient of unknown $\partial\omega/\partial p$ changes from 10^0 in the mass conservation law to $f_0 = 10^{-4}$ s^{-1} in the modified ζ equation, or the coefficient of $\partial\omega/\partial p$ possibly becomes $\zeta + f = 0$ if the assumption $\zeta + f \approx f$ is not used on the RHS of Eq. (3), causing additional $|\omega| \to \infty$. Observations show that $\zeta + f = 0$ could happen in the real atmosphere on the anticyclonic shear side of upper-layer jets in midlatitudes.

In order to explicitly consider all the mechanisms of ω (including $\nabla \cdot \boldsymbol{V}_2$), a full ω-mechanism equation (referred to as the full ω equation) can be derived by linearly combining the unsimplified vorticity equation, primitive thermodynamic equation, and continuity equation in isobaric coordinates, since these primitive equations are linear diagnostic equations for the only unknown ω (see the appendix). The linear combination of these primitive equations makes derivation simple, avoids reducing the order of magnitude for the coefficients of ω, avoids introducing fourth-order derivatives, and works for the global ω.

Since observational ω data are not available for determining the linear-combination-related coefficients (see the full ω equation in the appendix with c_1 for the primitive mass continuity equation, c_2 for the primitive thermodynamic equation and c_3 for the unsimplified vorticity equation), the ECMWF ω data were used as the "observed" ω data. According to Simmon and Burridge (1981), the ECMWF ω data are obtained from the mass continuity equation, which suggests that the error (i.e., the absolute value of the difference between the global-mean ω values from the ECMWF and from the full ω model) should approach zero with $c_2 \to 0$ and $c_3 \to 0$ (Fig. A1 in the appendix). Determining the unique-optimal $c_2 \neq 0$ and $c_3 \neq 0$ requires at least one designed in situ observation with intensive measurements and extra-high technologies. This in situ observation is as necessary as TOGA (Tropical Ocean–Global Atmosphere) designed for solving problems systematically.

Acknowledgements. This study was supported by the National Key Basic Research Project of China (Grant No. 2009CB 421404), the Chinese NSF key project (Grant Nos. 40930950 and 40730951), and the Chinese NSF (Grant Nos. 40775031 and 40575021).

APPENDIX A

A full ω global model with the explicit contribution of $\nabla \cdot \boldsymbol{V}_2$ to ω without fourth-order derivatives

Responsible for the vertical transport of mass, energy and momentum or vorticity, ω appears in many primitive (unsimplified) equations governing geophysical-fluid behaviors in the real atmosphere. These equations include the mass continuity equation in the spherical-isobaric coordinates (for diagnosing the global ω):

$$\frac{\partial\omega}{\partial p} = -\nabla \cdot \boldsymbol{V}_2 = -\left(\frac{\partial u}{\partial x} + \frac{1}{\cos\varphi}\frac{\partial v\cos\varphi}{\partial y}\right), \qquad \text{(A1)}$$

with $a = 6.37 \times 10^6$ m in $\partial x = a\cos\varphi\partial\lambda$ and $\partial y = a\partial\varphi$, where λ is the longitude and φ the latitude. The unknown ω also appears in the thermodynamic equation in terms of potential temperature θ:

$$-\sigma\omega = \frac{R\dot{Q}}{c_p p} - \frac{RT}{p}\left(\frac{\partial\ln\theta}{\partial t} + \boldsymbol{V}_2 \cdot \nabla\ln\theta\right), \qquad \text{(A2)}$$

where $\dot{Q}$ is the diabatic heating rate. The unsimplified relative-vorticity equation is obtained by applying the curl operator, $\{\partial(\,)/\partial\lambda - \partial[(\,)\cos\varphi]/\partial\varphi\}/(a\cos\varphi)$, to the primitive horizontal velocity equation, yielding

$$-\left(\frac{\partial\omega}{\partial x}\frac{\partial v}{\partial p} - \frac{\partial\omega}{\partial y}\frac{\partial u}{\partial p}\right) - \omega\frac{\partial\zeta}{\partial p}$$
$$= (\zeta + f)\nabla \cdot \boldsymbol{V}_2 + \boldsymbol{V}_2 \cdot \nabla\zeta + v\frac{df}{dy} + \frac{\partial\zeta}{\partial t} - \boldsymbol{k} \cdot \mathrm{curl}F, \qquad \text{(A3)}$$

where the relative vorticity in spherical coordinates is

$$\zeta = \frac{\partial v}{\partial x} - \frac{\partial(u\cos\varphi)}{\cos\varphi\partial y}$$

and the vertical component of the curl of frictional force, $\boldsymbol{F}$, is

$$\boldsymbol{k} \cdot \mathrm{curl}\boldsymbol{F} = \frac{\partial F_y}{\partial x} - \frac{\partial(F_x\cos\varphi)}{\cos\varphi\partial y}$$

in spherical coordinates. Similar to the $\omega_{\rm QG}$ equation, a full ω diagnostic equation should take into account all the geophysical-fluid-dynamic equations involving ω. Different from the $\omega_{\rm QG}$ equation, this full ω equation should be derived

without eliminating any ω term on the LHS of Eqs. (A1)–(A3) and introducing higher-order derivatives into the model for diagnosing the weak signal of ω.

We notice that in terms of the only unknown ω, Eqs. (A1)–(A3) are ω's linear (due to the absence of nonlinear terms of ω) and diagnostic (due to the absence of $\partial\omega/\partial t$) equations. Thus, the linear combination principle is applied to the incorporation of Eqs. (A1)–(A3), resulting in

$$L(\omega) = S, \tag{A4}$$

where

$$\begin{aligned} L(\omega) = {} & c_1\Omega\frac{\partial\omega}{\partial p} - c_3\left(\frac{\partial v}{\partial p}\frac{\partial\omega}{\partial x} - \frac{\partial u}{\partial p}\frac{\partial\omega}{\partial y}\right) - \\ & \left(c_3\frac{\partial\zeta}{\partial p} + c_2\Omega\sigma\right)\omega \\ S = {} & -\left[c_1\Omega - c_3(\zeta+f)\right]\nabla\cdot\boldsymbol{V}_2 + \\ & c_2\Omega\left[\frac{R\dot{Q}}{c_p p} - \frac{RT}{p}\left(\frac{\partial\ln\theta}{\partial t} + \boldsymbol{V}_2\cdot\nabla\ln\theta\right)\right] \\ & + c_3\left[\boldsymbol{V}_2\cdot\nabla\zeta + v\frac{df}{dy} + \frac{\partial\zeta}{\partial t} - \boldsymbol{k}\cdot\mathrm{curl}\boldsymbol{F}\right]. \end{aligned}$$

In the derivation of Eq. (A4), Eqs. (A1), (A2) and (A3) are respectively weighted by $c_1\Omega$, $c_2\Omega$ and c_3. If $c_1 = c_2 = \sqrt{2}$ is selected, then $c_1\Omega = c_2\Omega$ is equivalent to the Coriolis parameter, $f = 2\Omega\sin\varphi$, at $\varphi = 45^\circ$ latitude with $\Omega = 7.292\times10^{-5}$ s^{-1} for unit consistency. One of the advantages of Eq. (A4) is the absence of fourth-order derivatives since the weak signal of ω attributed to fourth-order-derivative terms [e.g., the RHS terms of Eq. (1)] might be masked by discrete, truncation and roundoff errors accompanying the use of computers, gridded data and finite difference schemes (e.g., Dunn, 1991; Press et al., 1992, p. 180; Räisänen, 1995). The second advantage is that $\nabla\cdot\boldsymbol{V}_2$ and all other ω-related mechanisms have been explicitly included in Eq. (A4), and the third is that all mechanisms are in their familiar forms with clear physical meanings given by primitive equations. As mentioned earlier, Eq. (A4) is derived for diagnosing the global ω.

The simplest way to handle the weighting functions in Eq. (A4) is to treat c_1, c_2 and c_3 as three constant parameters. The values of c_1, c_2 and c_3 can be determined by pursuing the best fit between the observed global ω and the global ω obtained from solving Eq. (A4). To solve Eq. (A4) numerically with the periodic boundary in the zonal direction and with the observed ω as meridional boundary values of ω, we apply the central difference scheme to Eq. (A4) and obtain the following finite difference equation:

$$\begin{aligned} & c_1\Omega\frac{\omega_{i,j,k+1}-\omega_{i,j,k}}{\Delta p} - c_3\frac{v_{i,j,k+1}-v_{i,j,k}}{\Delta p}\cdot\frac{(\omega_{i+1,j,k+1}-\omega_{i-1,j,k+1})+(\omega_{i+1,j,k}-\omega_{i-1,j,k})}{4\Delta x} + \\ & c_3\frac{u_{i,j,k+1}-u_{i,j,k}}{\Delta p}\cdot\frac{(\omega_{i,j+1,k+1}-\omega_{i,j-1,k+1})+(\omega_{i,j+1,k}-\omega_{i,j-1,k})}{4\Delta y} - \left(c_3\frac{\zeta_{i,j,k+1}-\zeta_{i,j,k}}{\Delta p} + c_2\Omega\sigma\right)\cdot \\ & \frac{1}{2}\left(\frac{\omega_{i+1,j,k+1}+\omega_{i-1,j,k+1}+\omega_{i,j+1,k+1}+\omega_{i,j-1,k+1}}{4} + \omega_{i,j,k}\right) = S_{i,j,k+\frac{1}{2}}\,, \end{aligned} \tag{A5}$$

where ω at level $k=1$ should be specified with the observed global ω. We use the four-point mean of ω in the last LHS term of Eq. (A5) to represent $\omega_{i,j,k+1}$ for ensuring the non-zero coefficient of $\omega_{i,j,k+1}$.

The Gauss–Seidel iteration method is used to solve Eq. (A5). To clearly explain the procedure of the Gauss–Seidel iteration (Haltiner and Williams, 1980, p. 156), we rewrite Eq. (A5) as

$$\omega^{(n+1)}_{i,j,k+1} = L(\omega^{(n+1)}_{i-1,j,k+1}, \omega^{(n+1)}_{i,j-1,k+1}, \omega^{(n)}_{i+1,j,k+1}, \omega^{(n)}_{i,j+1,k+1}, d)\,, \tag{A6}$$

where the superscript n represents the nth iteration, L represents a linear finite-difference operator and d includes all the known quantities as well as the ω available at the kth level with ω at $k=1$ given by the observations. At the beginning of the Gauss–Seidel iteration with $n=1$, the RHS ω values at level $k+1$ are also unknown. In order to start the iteration, we simply set them to arbitrary values such as $\omega^{(n+1)}_{i-1,j,k+1} = \omega^{(n+1)}_{i,j-1,k+1} = \omega^{(n)}_{i+1,j,k+1} = \omega^{(n)}_{i,j+1,k+1} = 0$. During the calculation based on Eq. (A6), the RHS ω values at level $k+1$ are updated immediately. This procedure is repeated with $n = 1, 2, \cdots$ until $|\omega^{(n+1)}_{i,j,k+1} - \omega^{(n)}_{i,j,k+1}| < 1.0\times10^{-3}$ Pa s^{-1}, yielding the ω field at level $k+1$. Using the ω field available at level $k+1$ and repeating the same iteration procedure, we obtain ω fields at levels $k+2, k+3, \cdots$.

Because the observed ω values are used as meridional boundary conditions and the lowest-level values of ω in this global model with the periodic boundary as the zonal boundary, determining non-zero c_1, c_2 and c_3 requires at least one designed in situ observation with international cooperation (for the global ω), technical innovation and enhanced monitoring with high-level technologies, among other factors. As mentioned in section 5, the observed global ω is not yet available. So far, we can only perform a theoretical justification of the full ω linear model with the ECMWF ω as the "true" ω. According to Simmons and Burridge (1981), the ECMWF ω is derived from the mass continuity equation, which indicates $c_1 \neq 0$ and $c_2 = c_3 = 0$ for the best fit between the global ω from the ECMWF and the global ω from Eq. (A6). This theoretical inference has been confirmed by numerical experiments with $c_1 = 10$, $c_2 \in [-4, 4]$, $c_3 \in [-3, 3]$ and $\Delta c_2 = \Delta c_3 = 1$ (Fig. A1) as well as with available values of $\nabla\cdot\boldsymbol{V}_2$, T, u and v etc. from the ECMWF dataset. These experiments are all freed from the modifications of observed data, while such data modifications are common in other ω models (e.g., Holton, 1979, p. 137, 2004, p. 165; Pauley and Nieman, 1992, p. 1113; Räisänen, 1995, p. 2450) for removing the $\omega\to\infty$ problem caused by the observed $\sigma \leqslant 0$

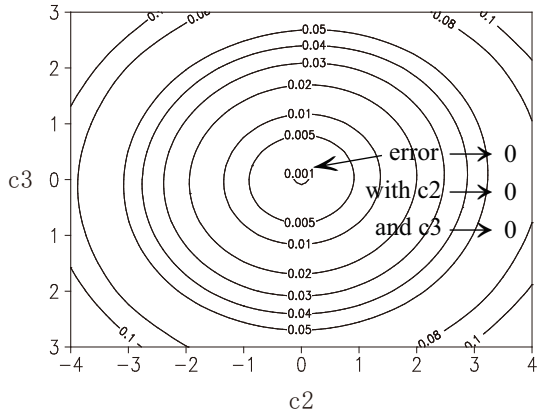

Fig. A1. The distribution of error as the function of c_2 and c_3. The error is the surface-to-100-hPa global-mean absolute value of the difference between ERA-40 global ω at 0600 UTC 27 January 1989 derived from the mass continuity equation (Simmons and Burridge, 1981) and the global ω from Eq. (A6). Therefore, the best fit should produce error$\rightarrow$0 with $c_2 \rightarrow 0$ and $c_3 \rightarrow 0$. In the numerical experiments based on the least-square fit method, the primitive continuity equation is weighted by Ωc_1 and $c_1 = 10$; the primitive thermodynamic equation is weighted by Ωc_2 and $c_2 \in [-4,4]$, i.e., the abscissa; and the unsimplified vorticity equation is weighted by c_3 and $c_3 \in [-3,3]$, i.e., the ordinate.

and $(\zeta + f)f \leqslant 0$.

REFERENCES

Dunn, L. B., 1991: Evaluation of vertical motion: Past, present, and future. *Wea. Forecasting*, **6**, 65–75.

Dutton, J. A., 1986: *The Ceaseless Wind: An Introduction to the Theory of Atmospheric Motion*. Dover Publications, 617 pp.

Haltiner, G. J., and R. T. Williams, 1980: *Numerical Prediction and Dynamic Meteorology*. 2nd ed. John Wiley & Sons Inc., 477 pp.

Holton, J. R., 1979: *An Introduction to Dynamic Meteorology*. 2nd ed., Academic Press, 391 pp.

Holton, J. R., 2004: *An Introduction to Dynamic Meteorology*. 4th ed., International Geophysics Series, Academic Press, 535 pp.

Hoskins, B. J., I. Draghici, and H. C. Davies, 1978: A new look at the ω-equation. *Quart. J. Roy. Meteor. Soc.*, **104**, 31–38.

Kim, B.-M., G.-H. Lim, and K.-Y. Kim, 2006: A new look at the midlatitude–MJO teleconnection in the northern hemisphere winter. *Quart. J. Roy. Meteor. Soc.*, **132**, 485–503.

Krishnamurti, T. N., 1968a: A diagnostic balance model for studies of weather systems of low and high latitudes, Rossby number less than 1. *Mon. Wea. Rev.*, **96**, 197–207.

Krishnamurti, T. N., 1968b: A study of a developing wave cyclone. *Mon. Wea. Rev.*, **96**, 208–217.

Pauley, P. M., and S. J. Nieman, 1992: A comparison of quasi-geostrophic and nonquasigeostrophic vertical motions for a model-simulated rapidly intensifying marine extratropical cyclone. *Mon. Wea. Rev.*, **120**, 1108–1134.

Petterssen, S., 1956: *Weather Analysis and Forecasting*. McGraw-Hill, 428 pp.

Press, W. H., S. A. Teukolsky, W. T. Vetterling, and B. P. Flannery, 1992: *Numerical Recipes in Fortran: The Art of Scientific Computing*. Combridge University Press, 933 pp.

Räisänen, J., 1995: Factors affecting synoptic-scale vertical motions: A statistical study using a generalized omega equation. *Mon. Wea. Rev.*, **123**, 2447–2460.

Simmons, A. J., and D. M. Burridge, 1981: An energy and angular-momentum conserving vertical finite-difference scheme and hybrid vertical coordinates. *Mon. Wea. Rev.*, **109**, 758–766.

Smith, P. J., 1971: An analysis of kinematic vertical motions. *Mon. Wea. Rev.*, **99**, 715–724.

Stone, M., and P. Goldbart, 2008: Mathematics for physics I. Pimander-Casaubon, 193–194. [Available online at http://webusers.physics.illinois.edu/∼m-stone5/mma/notes/amaster.pdf.]

Tan, Y.-C., and J. A. Curry, 1993: A diagnostic study of the evolution of an intense North American anticyclone during winter 1989. *Mon. Wea. Rev.*, **121**, 961–975.

Trenberth, K. E., 1978: On the interpretation of the diagnostic quasi-geostrophic omega equation. *Mon. Wea. Rev.*, **106**, 131–137.

Viúdez, Á., J. Tintoré, and R. L. Haney, 1996: About the nature of the generalized omega equation. *J. Atmos. Sci.*, **53**, 787–795.